Saturated fatty acid stimulates production of extracellular vesicles by renal tubular epithelial cells

Alyssa Cobbs[1] · Xiaoming Chen[1] · Yuanyuan Zhang[1] · Jasmine George[1] · Ming-bo Huang[2] · Vincent Bond[2] · Winston Thompson[1] · Xueying Zhao[1]

Abstract

Lipotoxicity, an accumulation of intracellular lipid metabolites, has been proposed as an important pathogenic mechanism contributing to kidney dysfunction in the context of metabolic disease. Palmitic acid, a predominant lipid derivative, can cause lipoapoptosis and the release of inflammatory extracellular vesicles (EVs) in hepatocytes, but the effect of lipids on EV production in chronic kidney disease remains vaguely explored. This study was aimed to investigate whether palmitic acid would stimulate EV release from renal proximal tubular epithelial cells. Human and rat proximal tubular epithelial cells, HK-2 and NRK-52E, were incubated with 1% bovine serum albumin (BSA), BSA-conjugated palmitic acid (PA), and BSA-conjugated oleic acid (OA) for 24–48 h. The EVs released into conditioned media were isolated by ultracentrifugation and quantified by nanoparticle-tracking analysis (NTA). According to NTA, the size distribution of EVs was 30–150 nm with similar mode sizes in all experimental groups. Moreover, BSA-induced EV release was significantly enhanced in the presence of PA, whereas EV release was not altered by the addition of OA. In NRK-52E cells, PA-enhanced EV release was associated with an induction of cell apoptosis reflected by an increase in cleaved caspase-3 protein by Western blot and Annexin V positive cells analyzed by flow cytometry. Additionally, confocal microscopy confirmed the uptake of lipid-induced EVs by recipient renal proximal tubular cells. Collectively, our results indicate that PA stimulates EV release from cultured proximal tubular epithelial cells. Thus, extended characterization of lipid-induced EVs may constitute new signaling paradigms contributing to chronic kidney disease pathology.

Keywords Extracellular vesicles · Lipotoxicity · Renal proximal tubules · Palmitic acid

Introduction

Chronic kidney disease (CKD) burdens 14% of the U.S. general population with nearly half of individuals concurrently diagnosed with diabetes or cardiovascular disease [1]. In type 2 diabetes, there are limited indicators in loss of kidney function in early stages. However, the progression of CKD is associated with symptoms including a reduction in glomerular filtration rate, persistent proteinuria, and hyperlipidemia [2, 3]. Of these, hyperlipidemia exacerbates conditions in the kidney via insulin resistance, cell apoptosis, and inflammation augmenting kidney dysfunction over years [4–6].

At baseline, lipids are essential to cellular function as components of their biological membranes, a major form of energy storage and a vital part of cell signaling. However, accumulation of lipids, especially saturated fatty acids and their metabolites, in non-adipose tissue produces lipotoxicity resulting in significant cellular dysfunction and injury [7]. Non-esterified or free fatty acids in plasma are bound to carrier proteins, mostly albumin [8]. In a healthy kidney, normal glomerular filtration barrier prevents the permeation of albumin and albumin-bound fatty acids. In diabetic kidney disease, the glomerular filtration barrier is damaged exposing tubular epithelial cells to high levels of albumin-bound fatty acids from circulation and filtrate. The increased cellular internalization of dominant saturated fatty acids, such as palmitic acid (PA), has shown contributions to kidney deterioration through apoptosis, mitochondrial superoxide

✉ Xueying Zhao
  xzhao@msm.edu

1 Department of Physiology, Morehouse School of Medicine, Atlanta, GA 30310, USA

2 Department of Microbiology, Biochemistry & Immunology, Morehouse School of Medicine, Atlanta, GA 30310, USA

generation and endoplasmic reticulum (ER) stress [9–11]. On the other hand, monounsaturated fatty acids, such as oleic acid (OA), exhibit anti-inflammatory properties and have the ability to regulate cell survival [12, 13]. The histological changes associated lipotoxicity, an accumulation of intracellular lipids, drives severe kidney injury primarily in the proximal tubular cells [14]. Understanding the differences in PA and OA accumulation and function in proximal tubular cells may shed light on mechanisms of renal lipotoxicity.

In recent years, there has been rapid growth of interest in extracellular vesicles (EVs) proposing their role in normal and pathophysiological conditions. EVs are nanometer-sized, membrane surrounded, cell-secreted molecules that carry special cargo utilized for signal transduction and intercellular communication. EVs have been established as efficient carriers of DNA, RNA, and proteins, with the ability to regulate cell function via gene expression in recipient cells [15]. It has been reported that lipid-induced toxicity in hepatocytes increases the release of EVs which activates an inflammatory phenotype in macrophages [16] and a fibrotic response in hepatic stellate cells [17]. Emerging research foreshadows EVs potential to communicate between cell populations; however, the characterization of EVs in lipid-induced kidney injury remains unclear. Therefore, in the current study, we investigated the effect of fatty acids on EV release from cultured renal proximal tubular cells.

Materials and methods

Reagents

Palmitic acid (PA), oleic acid (OA), bovine serum albumin (BSA, A7030, fatty acid free and essentially globulin free), and anti-β-actin antibody were purchased from Sigma-Aldrich (St. Louis, MO). Cell culture medium and reagents were from Life Technologies (Carlsbad, CA).

Cell culture and fatty acid treatment

Normal renal proximal tubular cell lines from rat (NRK-52E) and human (HK-2) were purchased from the American Type Culture Collection (Manassas, VA). The cells were cultured in DMEM/F12 supplemented with 5% fetal bovine serum, 100 U/ml penicillin, and 100 µg/ml streptomycin. Cells were subcultured (passage number < 30) once a week until reaching confluency.

For fatty acid treatment, BSA-conjugated PA and OA were prepared using a modified method described previously [18]. In brief, PA and OA were dissolved with ethanol and in serum-free DMEM/F12 medium containing 4% BSA. A final concentration of 1% BSA, 250–750 µM PA or

OA conjugated with BSA, and 0.25% ethanol was achieved through further dilutions. Doses of PA and OA were based on previous in vitro studies [18, 19]. PA (500–750 µM) is two to three times higher than normal circulating levels of PA and more representative of elevated fatty acid levels seen in patients with insulin resistance and diabetes [20, 21]. Control media prepared similarly contained ethanol in the absence (normal control), or presence of 1% BSA (BSA control). 90% confluent cells were then exposed to the experimental groups for 24–48 h.

MTT cell viability assay

NRK-52E cells were seeded into 96-well plates (5000 cells/per well) until they reached 70–80% confluency. Confluent cells were exposed to control or fatty acids for 24 h. 3-(4,5-dimethylthiazol-2-yl)-2,5-diphenyltetrazolium bromide from the Invitrogen Vybrant MTT Cell Proliferation Assay Kit (Carlsbad, California) was dissolved in phosphate buffer saline, added to each well and incubated for 4 h at 37 °C. Dimethyl sulfoxide was added to each well for 10 min at 37 °C. Cell absorbency was analyzed at 570 nm using SpectroMax M5 from Molecular Devices (Sunnyvale, CA) and SoftMax Pro 6.2.2 software.

Annexin V positive assessment of apoptosis

NRK-52E cells were seeded into 12-well dishes until they reached 80% confluency. Cells were treated with experimental groups and controls for 24 h. Cells were collected in 1.5 mL tubes and centrifuged at 1000 rpm for 5 min. The cell pellet was resuspended in Annexin V-FITC binding buffer, Annexin V-FITC and propidium iodide from the Annexin V-FITC Apoptosis Detection Kit (Sigma-Aldrich). Cells were incubated for 15 min in the dark at room temperature, and then subjected to apoptosis detection using Guava easyCyte flow cytometer and Guava Nexin software module from Millipore Sigma (St. Louis, MO).

EV isolation by ultracentrifugation

EVs were isolated from cell culture medium as previously described [22]. Briefly, conditioned medium was centrifuged at $2000 \times g$ for 30 min to remove cells and debris. Supernatant fractions were filtered using 0.22-µm pore size filters. Filtered cell-free medium was ultracentrifuged at $120,000 \times g$ for 120 min. The resulting EV pellet was washed once with PBS using the same ultracentrifugation conditions, followed by resuspension in PBS. EV protein concentration was assessed by the Bio-Rad DC protein assay (Richmond, CA).

Nanoparticle-tracking analysis (NTA)

Analysis of size distribution and concentration of EVs were performed using NanoSight LM10 with NTA2.3 from NanoSight Ltd. (Minton Park, UK) as previously described [23]. Particles were automatically tracked and sized based on Brownian motion and the diffusion coefficient. Control medium and filtered PBS were used as controls in this technique. The NTA measurement conditions were: temperature $= 21.0 \pm 0.5$ °C; viscosity $= 0.99 \pm 0.01$ Cp; frames per second $= 25$; measurement time $= 30$ s. The detection threshold was similar in all samples. Two recordings were performed for each sample.

Western blotting

Cell lysates and EV protein samples were denatured in sodium-dodecyl-sulfate polyacrylamide gel electrophoresis (SDS-PAGE) sample buffer by heating at 95 °C for 15 min. Criterion 4–20% TGX Precast Gels from Bio-Rad was used to separate the proteins and blotted as previously described. Blots were incubated with the primary antibodies, anti-Alix (Abcam, Cambridge, MA), anti-tumor susceptibility gene 101 protein (TSG101, Abcam), anti-CD63 (Santa Cruz, Santa Cruz, CA), anti-HSP70 (BD, San Jose, CA), and anti-cleaved caspase-3 (Cell Signaling, Danvers, MA), followed by goat or rat anti-Ig secondary antibodies. Specific bands were detected using enhanced chemiluminescent substrate from GE Healthcare (Piscataway, NJ) and visualized on the ImageQuant LAS 4000 imaging system from GE Healthcare. For total EV protein, Ponceau S red staining was used for loading control. β-actin was used as an internal control for cell lysates. Relative band intensity was measured densitometrically using ImageJ software.

Fluorescence microscopy

To evaluate fatty acid accumulation in renal tubular cells, BODIPY 493/503 from Life Technologies was performed as described previously [24]. Briefly, NRK-52E cells were treated with BSA, PA (250 μM), or OA (250 μM) for 24 h. The cells were washed with PBS, fixed in 4% paraformaldehyde, and stained with BODIPY 493/503. Stained NRK-52E cells were observed and imaged by a Leica confocal microscope.

To visualize the uptake of EVs into recipient cells, isolated EVs were resuspended in PBS. Approximately, 1.5×10^8 EVs from HK-2 cells were fluorescently labeled with Exo-Green from System Biosciences (San Juan Capistrano, CA) and EVs from NRK-52E were labeled with PKH26 (Sigma-Aldrich). HK-2 or NRK-52E recipient cells were cultured on a coverslip in a 6-well plate until they reached 70% confluency. Confluent cells were washed twice with serum-free medium, and then exposed to 100 μl of labeled EVs resuspended in serum-free medium for 16 h. Cells were fixed with 4% paraformaldehyde, stained with DAPI and imaged by a Leica confocal microscope.

Statistical analysis

Data are expressed as mean $\pm$ SEM. Student's t test was used for comparison between two groups. Comparisons among multiple groups were performed by one-way ANOVA followed by Newman–Keuls post hoc test. Statistical significance was set at $P < 0.05$.

Results

Intracellular lipid accumulation in NRK-52E cells treated with fatty acids

Unsaturated and saturated fatty acids have been reported to differentially influence membrane composition and lipid droplet formation in nonfat cells [25, 26]. Therefore, NRK-52E cells were first stained with BODIPY 493/503 for neutral lipids to visualize intracellular lipid droplets and to determine their size following OA or PA treatment. As shown in Fig. 1a, fluorescence microscopy revealed that OA increased the number of lipid droplets significantly more than PA, though PA also slightly increased lipid droplet numbers compared to BSA control in NRK-52E cells. Moreover, cells with perinuclear large lipid droplets were found almost exclusively in the OA treatment. In contrast, PA-treated cells displayed increased small intracellular lipids scattered throughout the cytoplasm (Fig. 1a).

PA but not OA induces apoptosis in NRK-52E cells

Because an accumulation of fatty acids and their metabolites within cells has been associated with cellular injury and dysfunction, we examined the effects of OA and PA on apoptosis in NRK-52E cells. As depicted in Fig. 1b, Western blot analysis showed a dose-dependent increase in cleaved caspase-3 in NRK-52E cells treated with PA (250–750 μM). PA-induced apoptosis was further confirmed by flow cytometry, showing a significant increase in Annexin V positive cells in the presence of 500 μM PA (Fig. 2a, b). In contrast, OA (500 μM) slightly reduced the percentage of apoptotic cells, although there is no statistical significance. As expected, MTT analysis detected a significant reduction of viability after NRK-52E cells were treated with 500 μM PA, whereas OA did not negatively impact cell viability (Fig. 2c).
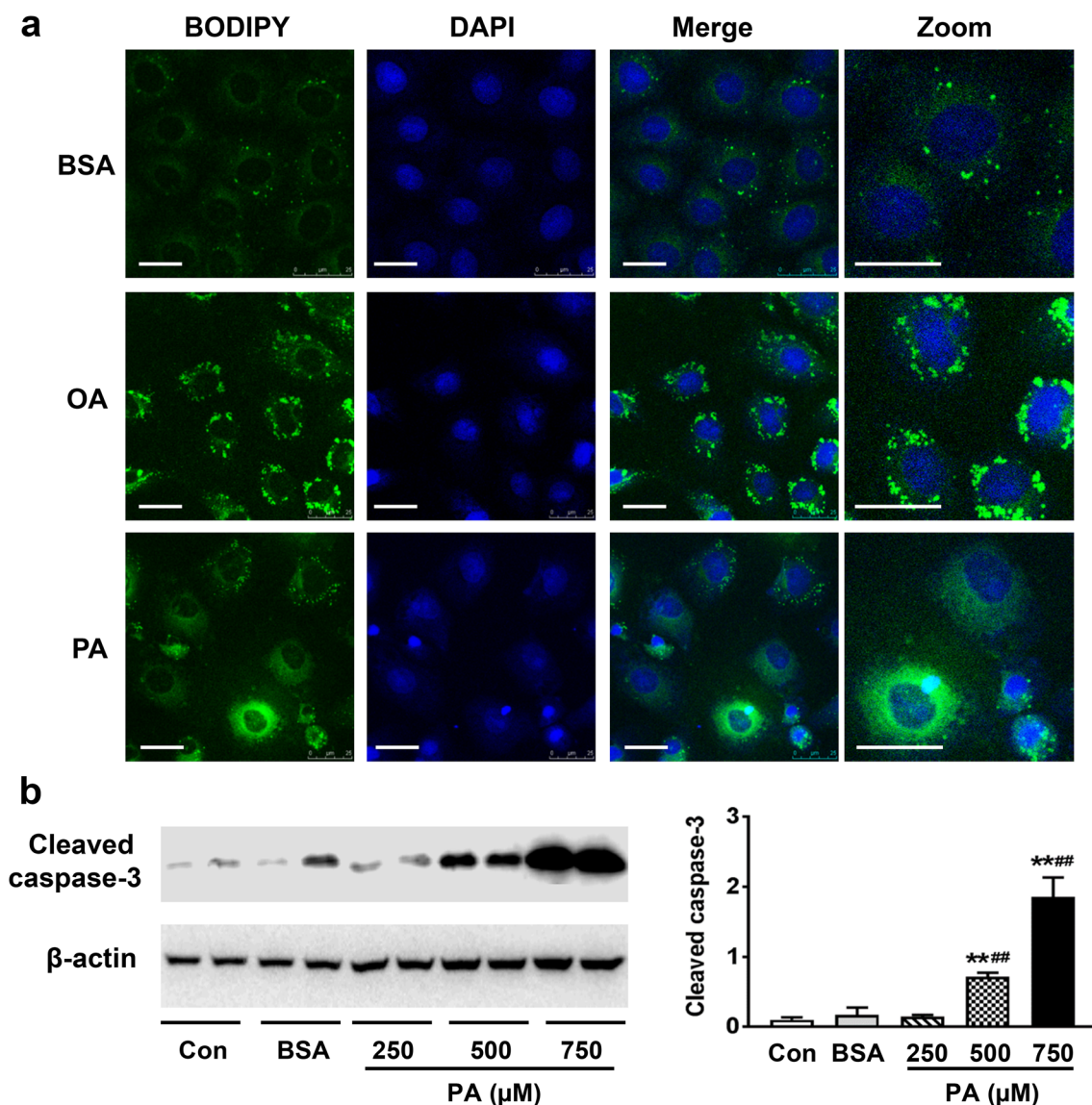
Fig. 1 Lipid accumulation and PA-induced caspase-3 activation in NRK-52E cells. **a** NRK-52E cells were treated with 1% BSA (BSA), BSA-conjugated palmitic acid (PA, 250 μM) or oleic acid (OA, 250 μM) for 24 h. Neutral lipids were stained with BODIPY 493/503 (green), and cell nuclei were stained with DAPI (blue). Bars: 25 μm. **b** Immunoblots for cleaved caspase-3 in NRK-52E cells treated with PA (250–750 μM) for 24 h. Image J was used to quantify band intensity of cleaved caspase-3 and normalized to β-actin. Data are expressed as mean ± SEM ($n = 3$–4). Statistical significance was indicated as **$P < 0.01$ and ##$P < 0.01$ versus normal control (Con) and albumin control (BSA), respectively. (Color figure online)

PA stimulated EV release from renal tubular epithelial cells

It has been shown that PA treatment accelerates EV production in hepatocytes and altered their miRNA profiles [17]. Next, we analyzed the EVs released from control and PA-treated NRK-52E cells to examine whether PA treatment also stimulates EV production in renal tubular cells. Based on NTA analysis, the size distribution of NRK-52E-derived EVs was 30–200 nm with a similar mode size (~ 50 nm) in all groups (Fig. 3a–c). Interestingly, a

24 h incubation of NRK-52E cells with BSA alone significantly increased EV amount compared to normal control (11.5×10^8 vs 2.9×10^8, $P < 0.01$) (Fig. 3d). When NRK-52E cells were exposed to 500 and 750 μM PA for 24 h, EV production was further increased to 23.1×10^8 ($P < 0.05$ compared to BSA control) and 30.2×10^8 ($P < 0.01$ compared to BSA control), respectively (Fig. 3d). Similarly, PA treatment also significantly increased EV production in HK cells (Fig. 4). Together, these results indicate that PA treatment stimulates the production of EVs in both rat and human proximal tubular cells.
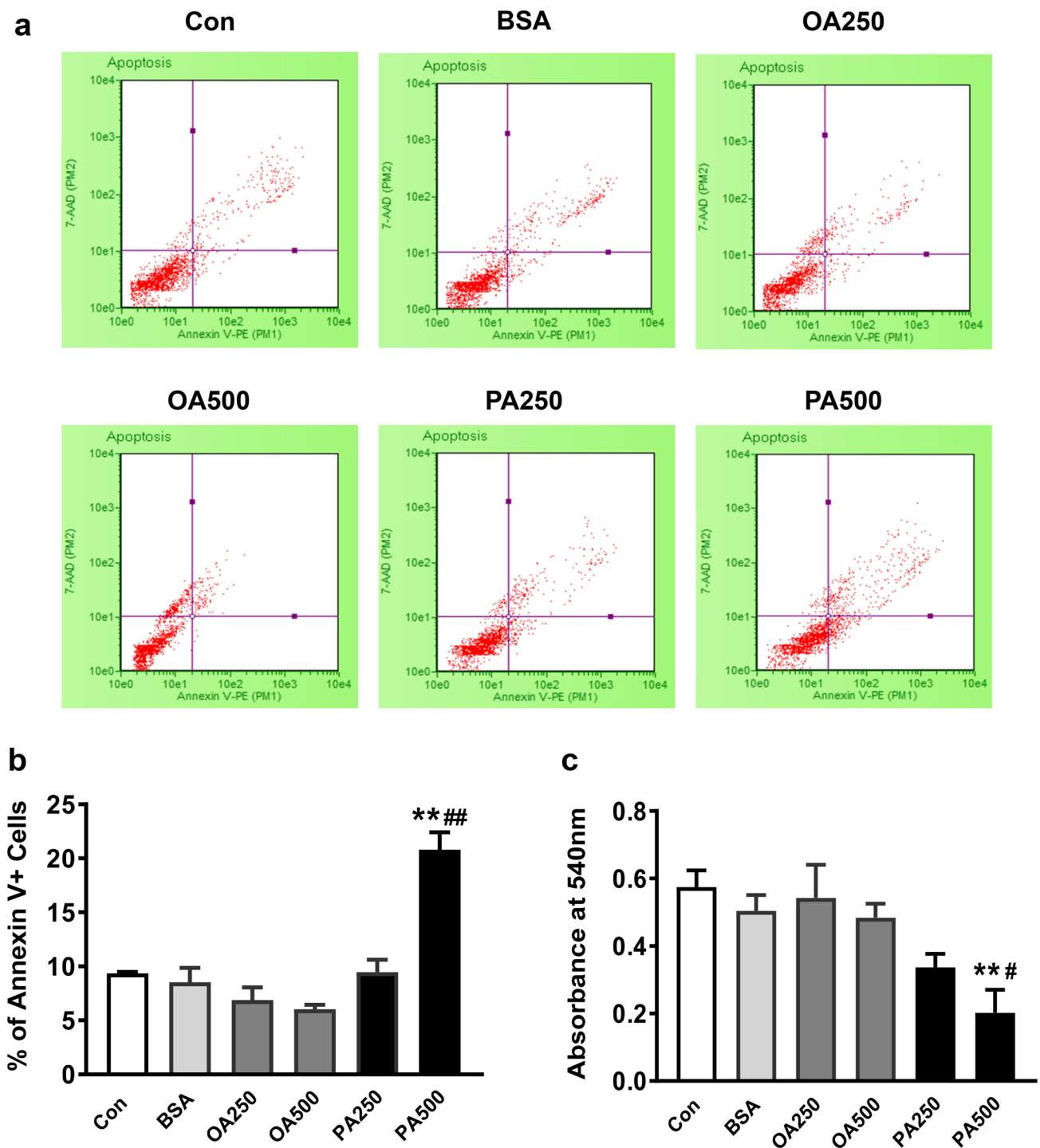
Fig. 2 The effect of fatty acids on apoptosis and cell viability in NRK-52E cells. NRK-52E cells were treated with Con, BSA or BSA-conjugated-OA or PA (250–500 μM) for 24 h. **a–b** FACS dot plots and quantification of NRK-52E cell apoptosis after 24 h treatment. Annexin V positive flow cytometry diagram depicts live, apoptotic and necrotic cells. The lower and upper right quadrants indicate the early and late apoptotic cells. The graph represents the percentage of early and late apoptotic cells detected by flow cytometry. **c** Cell viability was evaluated by an MTT assay. Data are expressed as mean ± SEM ($n = 4$). Statistical significances were defined at **$P < 0.01$ versus Con, #$P < 0.05$ and ##$P < 0.01$ versus BSA group
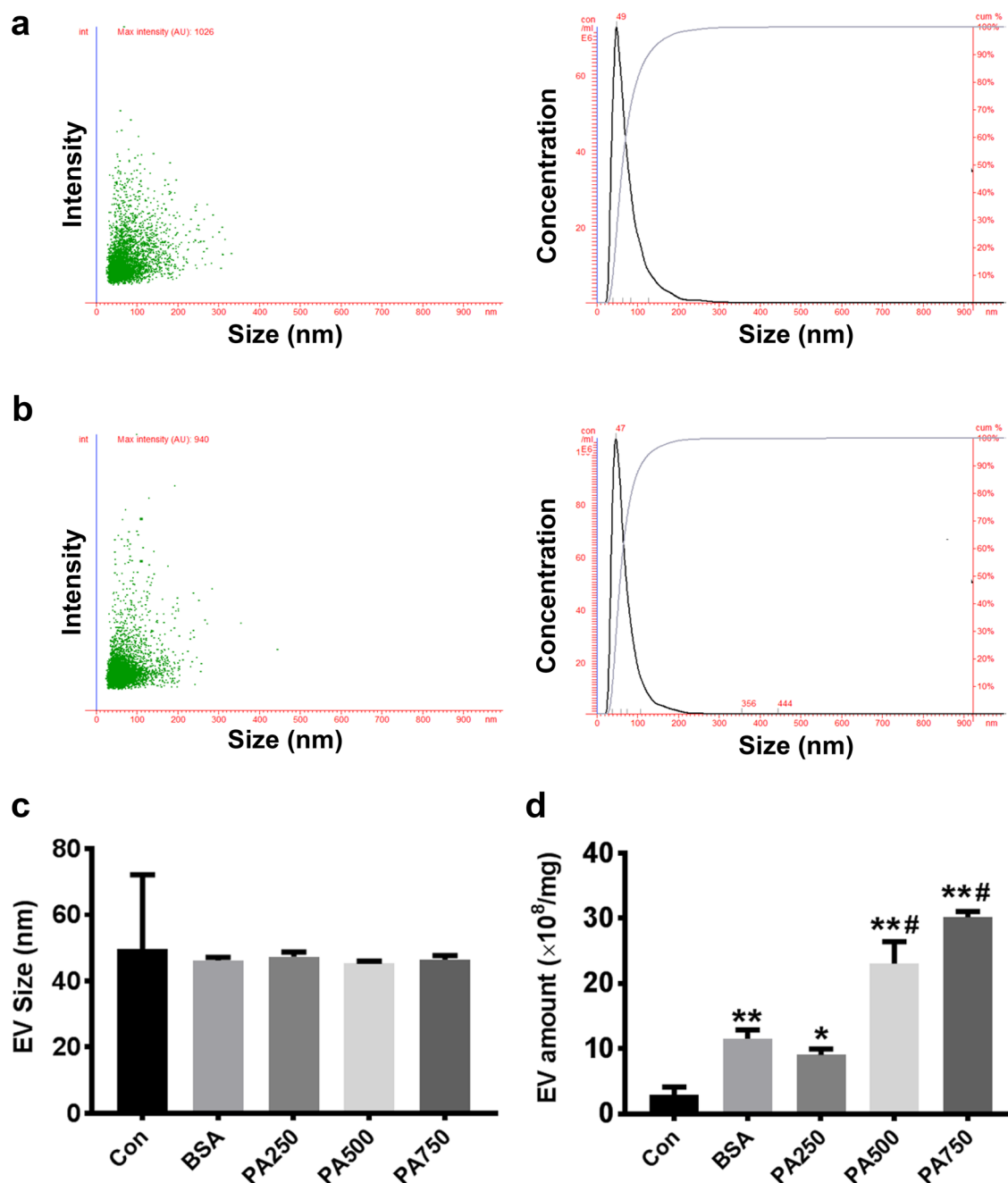
Fig. 3 PA stimulated EV release from NRK-52E cells. NRK-52E cells were treated with BSA or PA (250–750 μM) for 24 h. Nanoparticle-tracking analysis (NTA) was performed to characterize the EVs isolated from the conditioned media. **a–b** NTA graphs depict the intensity/concentration in relationship to the size distribution of EVs derived from NRK-52E cells treated with BSA (**a**) or 500 μM PA (**b**). **c–d** The averaged mode values (**c**) and concentration (**d**) of isolated EVs released from Con, BSA, and PA (250–500 μM)-treated NRK-52E cells. Data are expressed as mean $\pm$ SEM ($n=4$). *$P < 0.05$, **$P < 0.01$ versus Con; #$P < 0.05$, ##$P < 0.01$ versus BSA group

PA increased EV marker proteins Alix and TSG101

In combination with NTA, Western blot analysis for EV marker proteins was performed to further characterize EVs released from NRK-52E cells. As shown in Fig. 5, the isolated EVs and cells were probed for four proteins commonly enriched in EVs: Alix and TSG101, two proteins involved in the biogenesis of EVs; CD63, a member of tetraspanin protein family, and HSP70. We found that NRK-52E-derived EVs were enriched in Alix, TSG101 and HSP70. In contrast, CD63 was barely detectable in EVs derived from NRK-52E cells. To exclude the contamination with

Fig. 4 PA increased EV production at 24 and 48 h in HK-2 cells. HK-2 cells were treated with Con, BSA, PA (250 μM) and OA (250 μM). After 24 (**a**) and 48 (**b**) hours, EVs showed similar modes of size, 30–70 nm, among four groups. PA increased total amount of EVs released from HK-2 cells. Data are expressed as mean ± SEM ($n = 3$–6). $*P < 0.05$, $**P < 0.01$ versus Con; $^{##}P < 0.01$ versus BSA group
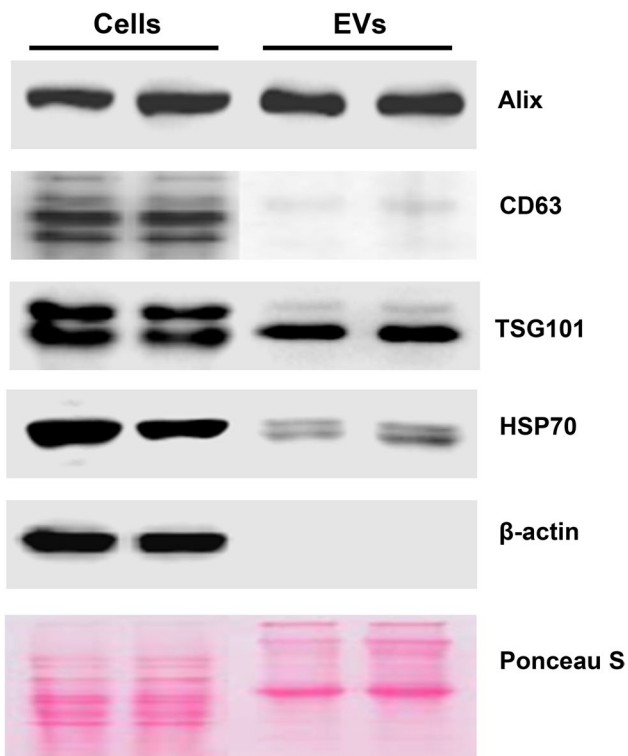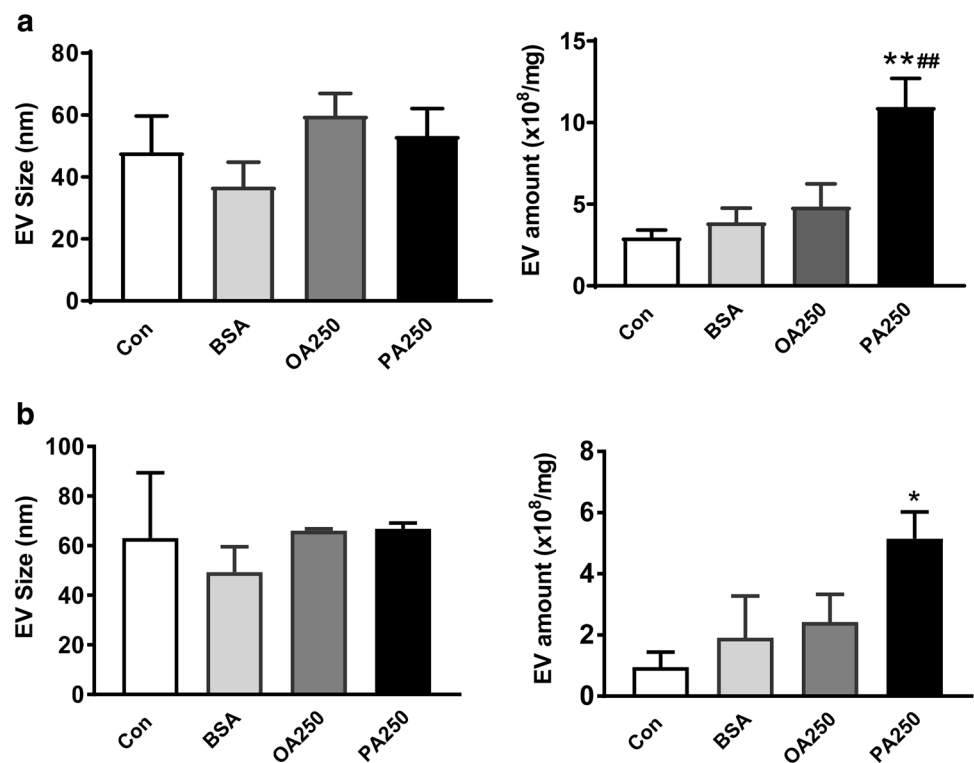

Fig. 5 Characterization of NRK-52E-derived EVs. Immunoblots detected EV marker proteins Alix, TSG101, CD63 and HSP70 in cell lysates and EV isolates. β-actin and Ponceau S staining was used as loading controls

intracellular organelles released via cell lysis, immunoblots for cytochrome c and lamin B2, markers for mitochondria and nuclear envelope, respectively, were also performed in NRK-52E-derived EVs. Neither cytochrome c nor lamin B2 was detected in isolated EVs (data not shown).

Next, we compared Alix and TSG101 protein levels in EVs isolated from BSA control and PA-treated NRK-52E cells. As depicted in Fig. 6, Alix and TSG101 proteins were increased in a dose-dependent manner when the cells were treated with 250–750 μM PA for 24 h. There was a close correlation between EV amount and marker protein levels ($r = 0.96$ for Alix and $r = 0.91$ for TSG101). Because the level of Alix and TSG101 was well correlated with the number of isolated EVs, we further evaluated the effect of OA on EV production by Western blot analysis. Both Alix and TSG101 proteins were not changed when NRK-52E cells were incubated with 500 μM OA for 24 h or 250 μM OA for 48 h, though increased EV marker proteins were observed in PA-treated cells (Fig. 7). These results confirmed that PA but not OA increased EV production in NRK-52E cells.

Autocrine uptake of lipid-induced EVs

In Fig. 8, we showed the uptake of tubular cell-derived EVs by HK-2 and NRK-52E cells. Isolated EVs were fluorescently labeled and co-cultured with HK-2 and NRK-52E recipient cells, respectively. After 16-h of incubation, confocal microscopy confirmed an uptake of EVs by the recipient
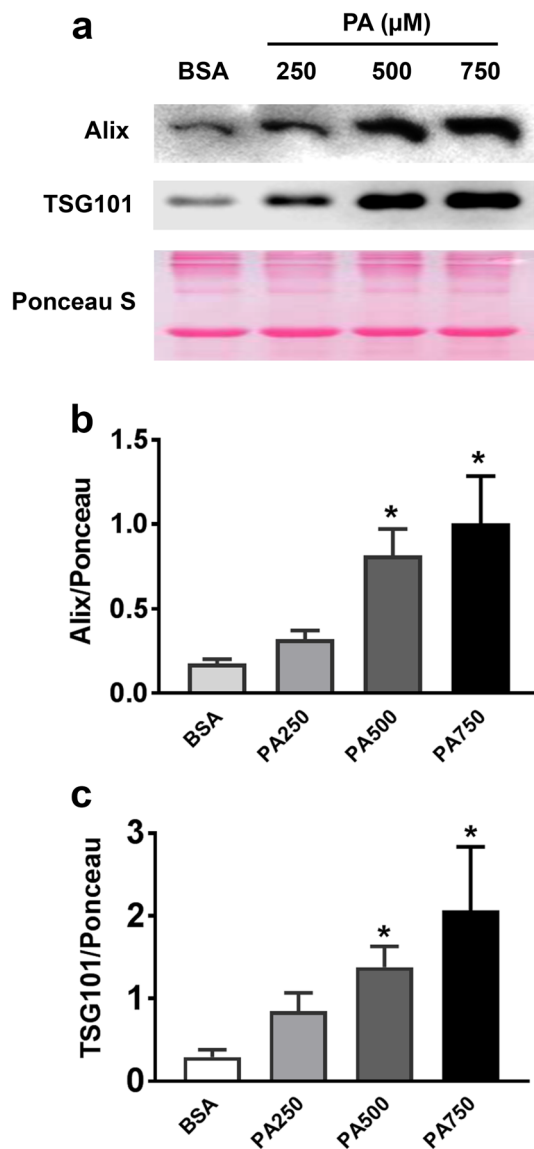
a

Fig. 6 PA increased Alix and TSG101 protein levels in EV derived from NRK-52E cells. NRK-52E cells were treated with or without PA for 24 h. **a** Representative Western blot images show a dose-dependent increase in Alix and TSG101 in EVs released from PA-treated cells. The Ponceau S staining was used as a loading control. **b–c** Image J was used to quantify band intensity of Alix and TSG101. Data are expressed as mean ± SEM ($n=3$). $^\#P<0.05$ versus BSA group
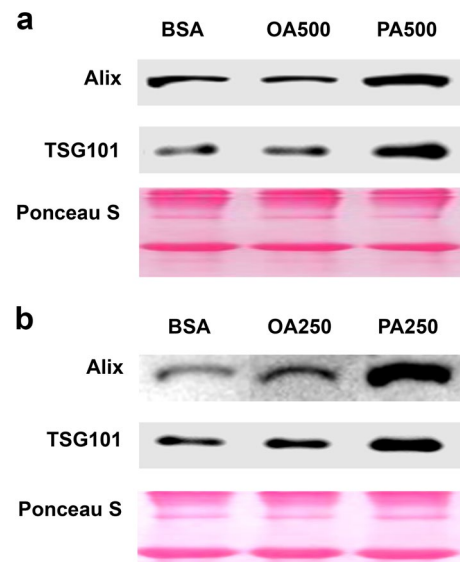
Fig. 7 PA but not OA increased Alix and TSG101 proteins in NRK-52E-derived EVs. **a** NRK-52E cells were treated with BSA, OA (500 μM) or PA (500 μM) for 24 h. **b** The cells were treated with BSA, OA (250 μM) or PA (250 μM) for 48 h. Immunoblots show that EV-related proteins Alix and TSG101 were not altered by 500 μM OA for 24 h or 250 μM OA for 48 h, though increased TSG101 and HSP70 protein level was observed in EVs derived from PA-treated cells

Increased intracellular lipid accumulation was accompanied by a reduction of cell viability and a profound increase in apoptosis in PA-treated NRK-52E cells. Moreover, PA treatment resulted in a dose-dependent increase in EV production in renal tubular cells. In contrast, OA did not significantly impact cell viability, apoptosis or EV production. Additionally, tubular cell-derived EVs may possess important functional potentials as demonstrated through an autocrine cellular uptake.

Differential regulations of cell membrane composition and lipid droplet formation by unsaturated and saturated FAs have been demonstrated in several nonfat cells [25–27]. For example, PA-treated cardiomyocytes [26] and mammary epithelial cells [25] exhibit marked differences in lipid histology compared to OA-treated cells. PA caused a diffused lipid-staining pattern, whereas OA led to the formation of noticeably large lipid droplets in cardiomyocytes and mammary epithelial cells. In line with these findings, BODIPY 493/503 staining of NRK-52E also revealed cell heterogeneity in all treatments with respect to presence and diameter of lipid droplets. NRK-52E cells exposed to OA contained large droplets, whereas PA-treated cells had poor lipid droplet formation despite an increase in lipid accumulation. Lipid droplets are pseudo-organelles essential for storage of excess intracellular lipids. Using differential ultracentrifugation of whole cardiomyocyte lysates on sucrose density gradients, Akoumi et al. [26]

cells. These results support a potential role of EVs in autocrine and paracrine communication.

Discussion

In the present study, we examined that saturated fatty acid PA but not unsaturated fatty acid OA stimulated cell apoptosis and EV production in renal proximal tubular cells.
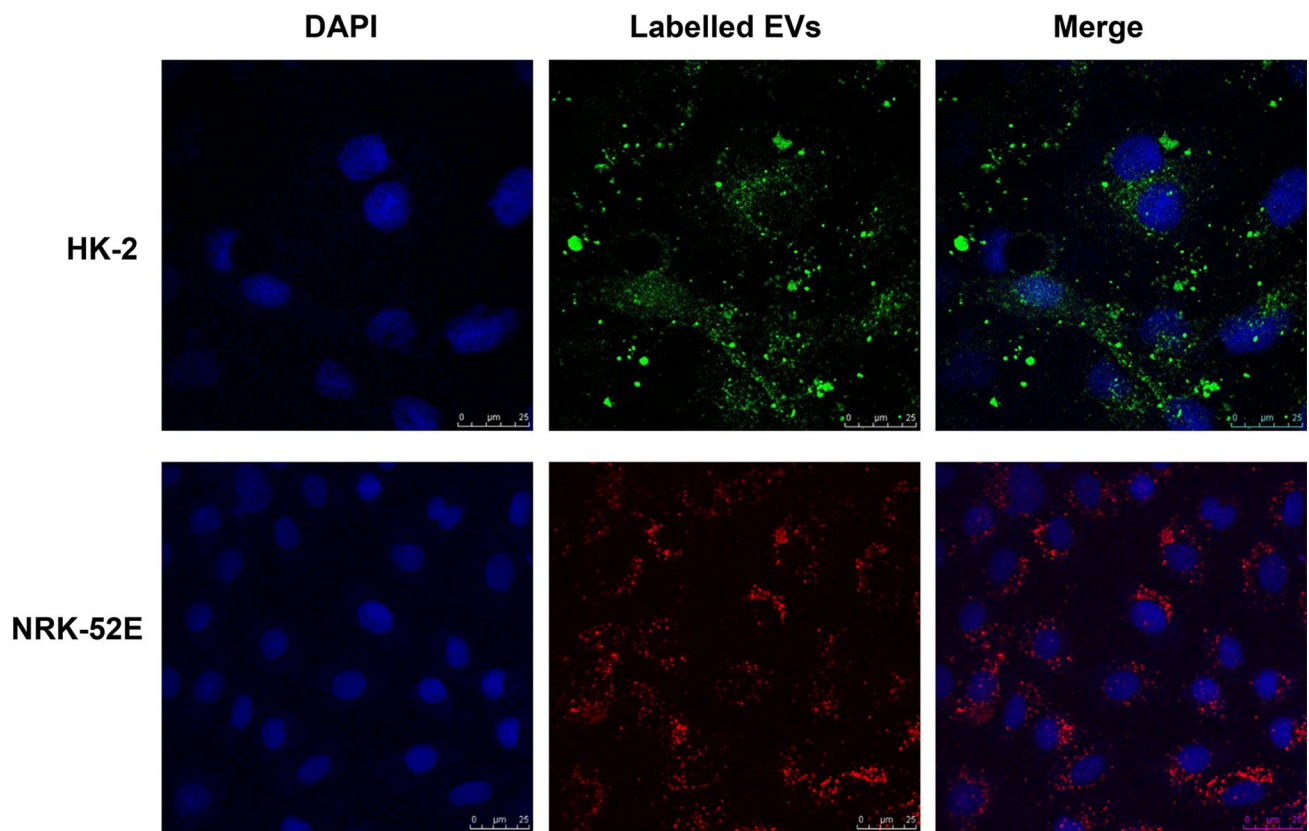
DAPI **Labelled EVs** **Merge**

Fig. 8 Uptake of tubular-derived EVs by HK-2 and NRK-52E cells. HK-2-derived EVs were fluorescently labeled with Exo-green and NRK-52E-derived EVs were fluorescently labeled with PKH26 (red), then incubated with HK-2 cells and NRK-52E cells, respectively. Cell nuclei were stained with DAPI (blue). Confocal microscopy was used to visualize the uptake of labeled EVs by HK-2 or NRK-52E cells. (Color figure online)

demonstrated that PA led to more lipid accumulation in the ER, while OA promoted more lipid accumulation in lipid droplets. In the absence of lipid droplets, lipid accumulation in the ER membrane causes ER stress and alterations of membrane integrity [26, 28]. Therefore, PA-induced lipid accumulation due to the lack of lipid droplet formation in renal tubular cells is likely a cause of cell damage and dysfunction.

Next, we investigated whether the difference in lipid histology induced by PA compared to OA was related to the difference in toxicity between these two FAs. Indeed, we found that PA administration caused a dose-dependent loss in cell viability, which was not observed in OA-treated NRK-52E cells. Moreover, PA treatment promoted cell apoptosis as evidenced by increased cleaved caspase-3 and Annexin V positive apoptotic cells. In contrast, OA slightly decreased the percentage of apoptotic cells. These results are consistent with the previous findings that PA caused oxidative and ER stress leading to apoptosis in proximal tubular cells [29]. Together, these results demonstrated the renal lipotoxic effects of saturated fatty acid PA, but not unsaturated fatty acid OA.

Recently, Hirvosa et al. have reported that lipid-induced signaling causes the release of inflammatory EVs from hepatocytes [16]. EVs are exfoliated membrane vesicles released into bodily fluids by most cell types. They are known to influence biological behaviors and are recognized as critical mediators of cell-to-cell communication in renal pathophysiology [30]. The production of EVs and their signature content is correlated with the progression and diagnosis of disease states such as endometriosis, nonalcoholic steatohepatitis and diabetic kidney disease [31–33]. Upon release, EVs interact with target cells that can result in the initiation of a myriad of signaling processes [34, 35]. This perspective implies that in addition to cellular stress and dysfunction, lipotoxicity may trigger changes in EV production and gene expression.

Thus, this study further validated the release of EVs in conditioned cell culture medium using a series of characterization techniques. NTA analysis allowed us to examine the number and the size of tubular cell-derived EVs in the absence or presence of fatty acids. Although the size distribution of EVs was not different in all groups, PA-treated proximal tubular cells are capable of releasing higher

amounts of EVs, compared to the other experimental groups. Next, we performed Western blots to determine the marker proteins enriched in NRK-52E-derived EVs. Our results revealed that Alix, TSG101 and HSP70 were abundant, but CD63 was barely detected in EVs derived from NRK-52E cells. These results suggest that Alix and TSG101 can serve as better markers for EVs released from renal proximal tubular cells. This concept was further supported by the demonstration of a close correlation between Alix and TSG101 protein level and EV amount. In the present study, we also found a significant increase in EV release when NRK-52E cells were stimulated with BSA alone, which is consistent with some previous reports. For example, it has been shown that EV production in rat proximal tubule cells was increased by fatty acid-free BSA (1 mg/ml) treatment and further elevated by advanced glycation end product-modified BSA [36]. Moreover, Lv et al. found that the chemokine CCL2 (MCP-1) mRNA, selectively enriched in the exosomes of mouse tubule epithelial cells after BSA stimulation, could be functionally delivered to the macrophages, culminating in macrophage activation and migration [37]. Similarly, studies performed in hepatocytes have demonstrated that EVs derived from PA-treated hepatocytes induce inflammatory response in macrophages [16] and fibrotic activation of hepatic stellate cells [17]. These studies also identified a potential link between hepatocyte lipotoxicity and macrophage mediated inflammation in nonalcoholic steatohepatitis (NASH). NASH and chronic kidney disease (CKD) have been shown to share common pathogenetic mechanisms regulating pathways involved in lipid metabolism, inflammation and fibrosis [38]. Therefore, we are leading the efforts to elucidate the roles of lipid-induced EVs in renal inflammation and fibrosis aimed at identifying probable CKD disease association and therapeutic implications.

To our knowledge, no one has mimicked lipotoxic conditions in kidney dysfunction and characterized EVs released from proximal tubular cells. Our observations suggest PA-mediated EV production could be dependent upon cellular apoptosis. In diseases like cancer, EVs released during a cell's apoptotic state (Apo-EVs) have shown important regulatory roles in communication with surrounding cells, as well as, activating or dampening immune response [39, 40]. Although a standard has not been defined, Apo-EVs display size varieties around 50 nm, whereas, apoptotic bodies have larger size characteristics commonly greater than 1000 nm [41]. EVs, perhaps including Apo-EVs, are capable of exerting specific functions in recipient cells facilitated by their cargo; implementing beneficial or detrimental functional changes. Given multiple modes by which EVs can interact with neighboring cells potential pathways can be targeted to elicit mechanisms by which Apo-EVs communicate with other lineages of cells [40]. As an approach to link functional activity with our lipid-induced EV isolates,

we fluorescently labeled HK-2 and NRK-52E EVs and demonstrated their autocrine uptake. Hence, we can conclude EV functional activity exists, although the nature of the function and effect on recipient cells needs further investigation. The work presented here sets a basis to further analyze the autocrine and paracrine roles of EVs derived from PA-treated proximal tubular cells.

Despite the efforts to date, the biological roles and cellular mechanisms underlying EV production during the onset and progression of CKD remains vague [42]. Due to EVs involvement in core disease-driven cellular processes, it is practical to elicit their biological functions including biogenesis, release, cell uptake, and transmission of cargo to target cells to inhibit disease progression [43]. In summary, we were able to prove that PA, a known mediator in the progression of CKD, stimulated the release of EVs in human and rat proximal tubular cells. Furthermore, our work supports the idea that EVs have functional potential by showing their uptake in recipient cells. Thus, lipid-induced EVs may serve as an untapped source to evaluate novel signaling pathways contributing to diabetic kidney disease progression.

Compliance with ethical standards

Conflict of Interest The authors declare no conflict of interest.

References

1. Saran R, Li Y, Robinson B, Abbott KC, Agodoa LY, Ayanian J, Bragg-Gresham J, Balkrishnan R, Chen JL, Cope E, Eggers PW, Gillen D, Gipson D, Hailpern SM, Hall YN, He K, Herman W, Heung M, Hirth RA, Hutton D, Jacobsen SJ, Kalantar-Zadeh K, Kovesdy CP, Lu Y, Molnar MZ, Morgenstern H, Nallamothu B, Nguyen DV, O'Hare AM, Plattner B, Pisoni R, Port FK, Rao P, Rhee CM, Sakhuja A, Schaubel DE, Selewski DT, Shahinian V, Sim JJ, Song P, Streja E, Kurella TM, Tentori F, White S, Woodside K, Hirth RA (2016) US Renal Data System 2015 Annual Data Report: Epidemiology of Kidney Disease in the United States, Am J Kidney Dis67: Svii, S1–Svii, 305. https://doi.org/10.1053/j.ajkd.2015.12.014

2. Hager MR, Narla AD, Tannock LR (2017) Dyslipidemia in patients with chronic kidney disease. Rev Endocr Metab Disord 18:29–40. https://doi.org/10.1007/s11154-016-9402-z

3. Herman-Edelstein M, Scherzer P, Tobar A, Levi M, Gafter U (2014) Altered renal lipid metabolism and renal lipid accumulation in human diabetic nephropathy. J Lipid Res 55:561–572. https://doi.org/10.1194/jlr.P040501

4. Jiang T, Wang XX, Scherzer P, Wilson P, Tallman J, Takahashi H, Li J, Iwahashi M, Sutherland E, Arend L, Levi M (2007) Farnesoid X receptor modulates renal lipid metabolism, fibrosis, and diabetic nephropathy. Diabetes 56:2485–2493. https://doi.org/10.2337/db06-1642

5. Ormazabal V, Nair S, Elfeky O, Aguayo C, Salomon C, Zuniga FA (2018) Association between insulin resistance and the

development of cardiovascular disease. Cardiovasc Diabetol 17:122. https://doi.org/10.1186/s12933-018-0762-4

6. Prieur X, Roszer T, Ricote M (2010) Lipotoxicity in macrophages: evidence from diseases associated with the metabolic syndrome. Biochim Biophys Acta 1801:327–337. https://doi.org/10.1016/j.bbalip.2009.09.017

7. Weinberg JM (2006) Lipotoxicity. Kidney Int 70:1560–1566. https://doi.org/10.1038/sj.ki.5001834

8. Stadler K, Goldberg IJ, Susztak K (2015) The evolving understanding of the contribution of lipid metabolism to diabetic kidney disease. Curr Diabetes Rep 15:40. https://doi.org/10.1007/s11892-015-0611-8

9. Hua W, Huang HZ, Tan LT, Wan JM, Gui HB, Zhao L, Ruan XZ, Chen XM, Du XG (2015) CD36 mediated fatty acid-induced podocyte apoptosis via oxidative stress. PLoS ONE 10:e0127507. https://doi.org/10.1371/journal.pone.0127507

10. Lee E, Choi J, Lee HS (2017) Palmitate induces mitochondrial superoxide generation and activates AMPK in podocytes. J Cell Physiol 232:3209–3217. https://doi.org/10.1002/jcp.25867

11. Sieber J, Lindenmeyer MT, Kampe K, Campbell KN, Cohen CD, Hopfer H, Mundel P, Jehle AW (2010) Regulation of podocyte survival and endoplasmic reticulum stress by fatty acids. Am J Physiol Renal Physiol 299:F821–F829. https://doi.org/10.1152/ajprenal.00196.2010

12. Chen X, Li L, Liu X, Luo R, Liao G, Li L, Liu J, Cheng J, Lu Y, Chen Y (2018) Oleic acid protects saturated fatty acid mediated lipotoxicity in hepatocytes and rat of non-alcoholic steatohepatitis. Life Sci 203:291–304. https://doi.org/10.1016/j.lfs.2018.04.022

13. Palomer X, Pizarro-Delgado J, Barroso E, Vazquez-Carrera M (2018) Palmitic and oleic acid: the Yin and yang of fatty acids in type 2 diabetes mellitus. Trends Endocrinol Metab 29:178–190. https://doi.org/10.1016/j.tem.2017.11.009

14. Cobbs A, Ballou K, Chen X, George J, Zhao X (2018) Saturated fatty acids bound to albumin enhance osteopontin expression and cleavage in renal proximal tubular cells. Int J Physiol Pathophysiol Pharmacol 10:29–38

15. Xu R, Greening DW, Zhu HJ, Takahashi N, Simpson RJ (2016) Extracellular vesicle isolation and characterization: toward clinical application. J Clin Invest 126:1152–1162. https://doi.org/10.1172/JCI81129

16. Hirsova P, Ibrahim SH, Krishnan A, Verma VK, Bronk SF, Werneburg NW, Charlton MR, Shah VH, Malhi H, Gores GJ (2016) Lipid-induced signaling causes release of inflammatory extracellular vesicles from hepatocytes. Gastroenterology 150:956–967. https://doi.org/10.1053/j.gastro.2015.12.037

17. Lee YS, Kim SY, Ko E, Lee JH, Yi HS, Yoo YJ, Je J, Suh SJ, Jung YK, Kim JH, Seo YS, Yim HJ, Jeong WI, Yeon JE, Um SH, Byun KS (2017) Exosomes derived from palmitic acid-treated hepatocytes induce fibrotic activation of hepatic stellate cells. Sci Rep 7:3710. https://doi.org/10.1038/s41598-017-03389-2

18. Lennon R, Pons D, Sabin MA, Wei C, Shield JP, Coward RJ, Tavare JM, Mathieson PW, Saleem MA, Welsh GI (2009) Saturated fatty acids induce insulin resistance in human podocytes: implications for diabetic nephropathy. Nephrol Dial Transplant 24:3288–3296. https://doi.org/10.1093/ndt/gfp302

19. Sabin MA, Stewart CE, Crowne EC, Turner SJ, Hunt LP, Welsh GI, Grohmann MJ, Holly JM, Shield JP (2007) Fatty acid-induced defects in insulin signalling, in myotubes derived from children, are related to ceramide production from palmitate rather than the accumulation of intramyocellular lipid. J Cell Physiol 211:244–252. https://doi.org/10.1002/jcp.20922

20. Mook S, Halkes CC, Bilecen S, Cabezas MC (2004) In vivo regulation of plasma free fatty acids in insulin resistance. Metabolism 53:1197–1201

21. Murea M, Freedman BI, Parks JS, Antinozzi PA, Elbein SC, Ma L (2010) Lipotoxicity in diabetic nephropathy: the potential role of fatty acid oxidation. Clin J Am Soc Nephrol 5:2373–2379. https://doi.org/10.2215/CJN.08160910

22. Nakamura K, Sawada K, Kinose Y, Yoshimura A, Toda A, Nakatsuka E, Hashimoto K, Mabuchi S, Morishige KI, Kurachi H, Lengyel E, Kimura T (2017) Exosomes promote ovarian cancer cell invasion through transfer of CD44 to peritoneal mesothelial cells. Mol Cancer Res 15:78–92. https://doi.org/10.1158/1541-7786.MCR-16-0191

23. Huang MB, Gonzalez RR, Lillard J, Bond VC (2017) Secretion modification region-derived peptide blocks exosome release and mediates cell cycle arrest in breast cancer cells. Oncotarget 8:11302–11315. https://doi.org/10.18632/oncotarget.14513

24. Baumann JM, Kokabee L, Wang X, Sun Y, Wong J, Conklin DS (2015) Metabolic assays for detection of neutral fat stores. Bio Protoc 5:12

25. Cohen BC, Shamay A, Argov-Argaman N (2015) Regulation of lipid droplet size in mammary epithelial cells by remodeling of membrane lipid composition-a potential mechanism. PLoS ONE 10:e0121645. https://doi.org/10.1371/journal.pone.0121645

26. Akoumi A, Haffar T, Mousterji M, Kiss RS, Bousette N (2017) Palmitate mediated diacylglycerol accumulation causes endoplasmic reticulum stress, Plin2 degradation, and cell death in H9C2 cardiomyoblasts. Exp Cell Res 354:85–94. https://doi.org/10.1016/j.yexcr.2017.03.032

27. Plotz T, Hartmann M, Lenzen S, Elsner M (2016) The role of lipid droplet formation in the protection of unsaturated fatty acids against palmitic acid induced lipotoxicity to rat insulin-producing cells. Nutr Metab (Lond) 13:16. https://doi.org/10.1186/s12986-016-0076-z

28. Borradaile NM, Han X, Harp JD, Gale SE, Ory DS, Schaffer JE (2006) Disruption of endoplasmic reticulum structure and integrity in lipotoxic cell death. J Lipid Res 47:2726–2737. https://doi.org/10.1194/jlr.M600299-JLR200

29. Katsoulieris E, Mabley JG, Samai M, Sharpe MA, Green IC, Chatterjee PK (2010) Lipotoxicity in renal proximal tubular cells: relationship between endoplasmic reticulum stress and oxidative stress pathways. Free Radic Biol Med 48:1654–1662. https://doi.org/10.1016/j.freeradbiomed.2010.03.021

30. Pomatto MAC, Gai C, Bussolati B, Camussi G (2017) Extracellular vesicles in renal pathophysiology. Front Mol Biosci 4:37. https://doi.org/10.3389/fmolb.2017.00037

31. Ban LA, Shackel NA, McLennan SV (2016) Extracellular vesicles: a new frontier in biomarker discovery for non-alcoholic fatty liver disease. Int J Mol Sci 17:376. https://doi.org/10.3390/ijms17030376

32. Harp D, Driss A, Mehrabi S, Chowdhury I, Xu W, Liu D, Garcia-Barrio M, Taylor RN, Gold B, Jefferson S, Sidell N, Thompson W (2016) Exosomes derived from endometriotic stromal cells have enhanced angiogenic effects in vitro. Cell Tissue Res 365:187–196. https://doi.org/10.1007/s00441-016-2358-1

33. Yamamoto CM, Murakami T, Oakes ML, Mitsuhashi M, Kelly C, Henry RR, Sharma K (2018) Uromodulin mRNA from urinary extracellular vesicles correlate to kidney function decline in type 2 diabetes mellitus. Am J Nephrol 47:283–291. https://doi.org/10.1159/000489129

34. Dominguez JM, Dominguez JH, Xie D, Kelly KJ (2018) Human extracellular microvesicles from renal tubules reverse kidney ischemia-reperfusion injury in rats. PLoS ONE 13:e0202550. https://doi.org/10.1371/journal.pone.0202550

35. Gutierrez-Vazquez C, Villarroya-Beltri C, Mittelbrunn M, Sanchez-Madrid F (2013) Transfer of extracellular vesicles during immune cell-cell interactions. Immunol Rev 251:125–142. https://doi.org/10.1111/imr.12013

36. De S, Kuwahara S, Hosojima M, Ishikawa T, Kaseda R, Sarkar P, Yoshioka Y, Kabasawa H, Iida T, Goto S, Toba K, Higuchi Y, Suzuki Y, Hara M, Kurosawa H, Narita I, Hirayama Y, Ochiya T,

Saito A (2017) Exocytosis-mediated urinary full-length megalin excretion is linked with the pathogenesis of diabetic nephropathy. Diabetes 66:1391–1404. https://doi.org/10.2337/db16-1031

37. Lv LL, Feng Y, Wen Y, Wu WJ, Ni HF, Li ZL, Zhou LT, Wang B, Zhang JD, Crowley SD, Liu BC (2018) Exosomal CCL2 from tubular epithelial cells is critical for albumin-induced tubuloint-erstitial inflammation. J Am Soc Nephrol 29:919–935. https://doi.org/10.1681/ASN.2017050523

38. Musso G, Cassader M, Cohney S, De MF, Pinach S, Saba F, Gambino R (2016) Fatty liver and chronic kidney disease: novel mechanistic insights and therapeutic opportunities. Diabetes Care 39:1830–1845. https://doi.org/10.2337/dc15-1182

39. Caruso S, Poon IKH (2018) Apoptotic cell-derived extracellular vesicles: more than just debris. Front Immunol 9:1486. https://doi.org/10.3389/fimmu.2018.01486

40. Lynch C, Panagopoulou M, Gregory CD (2017) Extracellular vesicles arising from apoptotic cells in tumors: roles in cancer pathogenesis and potential clinical applications. Front Immunol 8:1174. https://doi.org/10.3389/fimmu.2017.01174

41. Atkin-Smith GK, Poon IKH (2017) Disassembly of the dying: mechanisms and functions. Trends Cell Biol 27:151–162. https://doi.org/10.1016/j.tcb.2016.08.011

42. Zhang W, Zhou X, Zhang H, Yao Q, Liu Y, Dong Z (2016) Extra-cellular vesicles in diagnosis and therapy of kidney diseases. Am J Physiol Renal Physiol 311:F844–F851. https://doi.org/10.1152/ajprenal.00429.2016

43. Lu CC, Ma KL, Ruan XZ, Liu BC (2017) The emerging roles of microparticles in diabetic nephropathy. Int J Biol Sci 13:1118–1125. https://doi.org/10.7150/ijbs.21140